ResearchGate

See discussions, stats, and author profiles for this publication at: https://www.researchgate.net/publication/15702891

Antimicrobial Peptide Pores in Membranes Detected by Neutron In-Plane Scattering

ARTICLE *in* BIOCHEMISTRY · JANUARY 1996

Impact Factor: 3.02 · DOI: 10.1021/bi00048a002 · Source: PubMed

CITATIONS
138

READS
14

4 AUTHORS, INCLUDING:

Steven J Ludtke
Baylor College of Medicine
127 PUBLICATIONS **7,864** CITATIONS

SEE PROFILE

Available from: Steven J Ludtke
Retrieved on: 02 February 2016

Accelerated Publications

Antimicrobial Peptide Pores in Membranes Detected by Neutron In-Plane Scattering†

Ke He, Steve J. Ludtke, and Huey W. Huang*

Physics Department, Rice University, Houston, Texas 77251-1892

David L. Worcester

Biology Division, University of Missouri, Columbia, Missouri 65211

Received September 5, 1995; Revised Manuscript Received October 24, 1995⊗

ABSTRACT: Antimicrobial peptides isolated from the host defense systems of animals have been shown to exert their activity directly on the lipid bilayer of cell membranes, but the antimicrobial mechanisms are not clear, due chiefly to the difficulty of discerning the high-order structures formed by these peptides in membranes. Previously we have shown that these peptides insert into the membrane when their concentrations exceed a lipid-dependent critical value. With neutron in-plane scattering we now show that inserted alamethicin creates aqueous pores ≳18 Å in diameter. The density of pores is consistent with the assumption that all of the alamethicin is involved in pore formation. Pores were not detected below the critical concentration. Thus concentration-dependent pore formation appears to be the molecular mechanism of antimicrobial action.

In the past 15 years a new class of antimicrobials in the form of small peptides has been discovered in the host defense systems of animals (Hultmark et al., 1980; Zasloff, 1987; Boman et al., 1994). Unlike the conventional antibiotics that have specific protein targets, these peptides have been shown to exert their activity directly on the lipid bilayer of the cellular membrane. However, extensive *in vitro* and *in vivo* studies have not clarified the primary mechanism by which bacteria are killed, except that it is generally agreed that binding of peptide monomers to the surface of the target cells causes disruption, permeabilization, or disintegration of cytoplasmic membranes (Boman et al., 1994). The situation reflects the poorly understood interactions between peptides and lipids. One major problem is that there isn't a good technique with which to visualize structures formed by these peptides in membranes. In this communication we describe a neutron in-plane scattering technique that addresses this problem. With this technique, we directly observed pores formed by alamethicin in lipid bilayers. The pores have a water pathway ≳18 Å in diameter. This and recent X-ray diffraction experiments clarify the mode of action of these peptides.

Among the antimicrobial peptides, the best studied are those that assume an amphipathic helical configuration when associated with a membrane, such as cecropins (Hultmark et al., 1980) and magainins (Zasloff, 1987). The orientation of helical peptides in membranes can be conveniently detected by oriented circular dichroism (Wu et al., 1990). We have found that all amphipathic helical peptides we have investigated, including magainins (Ludtke et al., 1994) and cecropins (unpublished experiments), associate with membranes in two ways. Depending on the conditions, they either adsorb parallel to the membrane surface or insert perpendicularly into the bilayer (Bechinger et al., 1991; Huang & Wu, 1991; Ludtke et al., 1994). Most surprisingly, these two states separate into two phases. In general, low concentration states are in the surface phase, and high concentration states are in the inserted phase, with a coexistence region in between. There is a reproducible, well-defined concentration marking the beginning of the coexistence region from the low concentration side (we will call it the critical concentration for insertion or CCI).[1] The low concentration phase is where the single-channel activities of the peptides are detected (Christensen et al., 1988; Duchohier et al., 1989; Cruciani et al., 1992), indicating that a very small fraction of the peptides may be inserted,[2] particularly if there is a transmembrane electric potential because helical peptides possess a dipole (Baumann & Mueller, 1974). However, since the single channels are transient fluctuation phenomena and there are repair mechanisms operating, cells may not be killed at low peptide concentrations (Boman et

† This work was supported in part by the National Institutes of Health Grant AI34367 and Biophysics Training grant GM08280, by Department of Energy Grant DE-FG03-93ER61565, and by the Robert A. Welch Foundation. The facility at the IPNS is funded by the Department of Energy, BES-Materials Science, under Contract W-31-109-Eng-38. Use of Rice University Intel iPSC/860 for simulations was provided by the Center for Research on Parallel Computation under NSF Cooperative Agreement Nos. CCR-8809615 and CDA-8619893 with support from the Keck Foundation.

* To whom correspondence should be addressed. Telephone: 713-527-4899. Fax: 713-527-9033. E-mail: Huang@ion.rice.edu.

⊗ Abstract published in *Advance ACS Abstracts,* November 15, 1995.

[1] Abbreviations: CCI, critical concentration for insertion; DLPC, 1,2-dilauroyl-*sn*-glycero-3-phosphatidylcholine; DPhPC, 1,2-diphytanoyl-*sn*-glycero-3-phosphatidylcholine.

[2] Other evidence for insertion was given by Matsuzaki et al. (1995).

0006-2960/95/0434-15614$09.00/0 © 1995 American Chemical Society

al., 1994). We hypothesized that at concentrations below CCI the peptides are nonlethal and that lysis occurs only if the peptide concentration exceeds CCI (Ludtke et al., 1994). Indeed, many investigators have observed sigmoidal concentration dependence in dose−responses that characterizes the cooperative nature of peptides' activity (Steiner et al., 1988; Juretic et al., 1989; Westerhoff et al., 1989; Cruciani et al., 1991; Gomes et al., 1993), consistent with having a minimum concentration for lysis. Furthermore, we have found that, for a given peptide, the CCI varies greatly with the lipid composition of the membrane (Huang & Wu, 1991; Ludtke et al., 1994). Thus there is a plausible explanation for the cell-type selectivity exhibited by host defense peptides, because cell membranes do have specific lipid compositions.

Spectroscopic methods such as solid-state NMR (Bechinger et al., 1991) and oriented circular dichroism (Wu et al., 1990) detect only the orientation of individual peptides in a membrane, leaving the high-order structures of the peptides unresolved. Recently, we have used X-ray diffraction to study the low concentration states. We found that the peptide monomers are adsorbed in the interfacial region of the lipid bilayer and their in-plane distribution is dispersed (rather than aggregated). The main effect of the peptide adsorption is reducing the thickness of the hydrocarbon region directly proportional to the peptide concentration (Wu et al., 1995; Ludtke et al., 1995). This has the effect of increasing the free energy of adsorption proportional to the square of the peptide concentration, which makes peptide insertion energetically favorable above a critical concentration (Huang, 1995).

The high-order structures of the inserted peptide were investigated by neutron scattering. Due to the large quantity of peptide needed for this study, we used alamethicin, an amphipathic helical peptide produced by fungi (Pandey et al., 1977). Although there are some important differences between alamethicin and the host defense peptides [i.e., the former is hemolytic (Jen et al., 1987) and the latter are not],[3] their interactions with lipid bilayers are similar. Specifically, alamethicin and magainin have similar concentration dependence of orientation as described above (Huang & Wu, 1991; Ludtke et al., 1994), and their effects on lipid bilayers at low concentrations are also similar (Wu et., 1995; Ludtke et al., 1995). Thus, the alamethicin results should shed light on the mode of action of host defense peptides.

MATERIALS AND METHODS

1,2-Dilauroyl-*sn*-glycero-3-phosphatidylcholine (DLPC) and 1,2-diphytanoyl-*sn*-glycero-3-phosphatidylcholine (DPhPC) in $CHCl_3$ were purchased from Avanti Polar Lipids, Inc. (Alabaster, AL). Alamethicin was purchased from Sigma Chemical Co. (St. Louis, MO). Alamethicin is a mixture of components, principally alamethicin I (85% by HPLC) and alamethicin II (12%), which differ by one amino acid (Pandey et al., 1977). Both lipid and peptide were used without further purification. Alamethicin and lipid at the desired peptide/lipid molar ratio (P:L) were first codissolved in chloroform/methanol. The solvent was removed by a slow nitrogen purge followed by drying under vacuum (10 μm) for at least 20 h. D_2O was added to the peptide−lipid film. The mixture was homogenized with a sonicator so as to break up large aggregates. The lipid/peptide dispersion was lyophilized. The lyophilized powder was then hydrated with D_2O vapor. Control samples, i.e., lipid without peptide, were similarly prepared. Quartz plates of 0.25 mm in thickness were purchased from Chemglass, Inc. (Vineland, NJ). They were cleaned with hot sulfuric/chromic acid and then thoroughly rinsed with distilled water before use.

At room temperature the fully hydrated peptide/lipid mixtures were in the liquid crystalline phase (Wu et al., 1995). They were aligned into parallel multilayers between thin quartz plates (Asher & Pershan, 1977; Huang & Olah, 1987). The peptide orientation was monitored by oriented circular dichroism (Wu et al., 1990). For P:L $\geq$ 1:15, alamethicin in DPhPC is in the inserted phase (CCI $\sim$ 1:40; Wu et al., 1995). On the other hand, the inserted phase of alamethicin in DLPC extends to as low as at least P:L $\sim$ 1:200, the limit of the oriented circular dichroism technique (Huang & Wu, 1991). Six thin layers of D_2O-hydrated sample were held between seven parallel plates. The total sample thickness was about 0.25 mm. The sample area was about 1.5 cm in diameter. It was possible to examine the condition of each layer under a polarized microscope. Visual inspection allowed us to determine that the lipid was in the smectic liquid crystalline state (Asher & Pershan, 1977; Huang & Olah, 1987). One signature of the smectic phase is the presence of oily streaks (see the inset of Figure 2 below). These inevitable smectic defects in multilayer samples give rise to lamellar diffraction peaks during measurement of in-plane scattering. The lamellar peak allows us to monitor the hydration and other conditions of the sample, but it must be small (few smectic defects) for good measurement of the in-plane scattering.

Neutrons were scattered off the samples with the momentum transfer **Q** oriented parallel to the multilayers. For $Q < 0.5$ Å^{-1}, in-plane scattering can be conveniently performed in a standard small-angle scattering facility with the multilayer sample oriented normal to the incident neutron beam. The experiment was performed at the Intense Pulsed Neutron Source (IPNS), Argonne National Laboratory, using the Small Angle Diffractometer. Preliminary experiments were performed at the Cold Neutron Research Facility, National Institute of Standards and Technology (NIST), using the NG-7 30-meter Small Angle Neutron Scattering Instrument and at the University of Missouri Research Reactor.

RESULTS

Figure 1 shows a typical neutron in-plane scattering of DLPC bilayers containing inserted alamethicin and hydrated with D_2O. Figure 2 shows neutron in-plane scattering of a control sample, i.e., oriented bilayers of pure lipid hydrated with D_2O. The scattering curve of pure lipid consists of only a sharp peak at $Q = 0.12$Å^{-1} on the top of a constant background. A similar peak also appears in Figure 1. These are due to the smectic defects mentioned above. If the bilayers were perfectly aligned and free of smectic defects, the in-plane scattering of pure lipid multilayers would be a sum of the scattering of D_2O and of lipid molecules. For the liquid state, this scattering should have no significant Q

[3] The host-defense peptides, such as cecropins and magainins, are cationic. Alamethicin is neutral or slightly anionic (Pandely, 1977). However, the charges alone are not the determinant of the cell-type specificity. Melittin is cationic, similar to magainins and cecropins, but it is hemolytic.

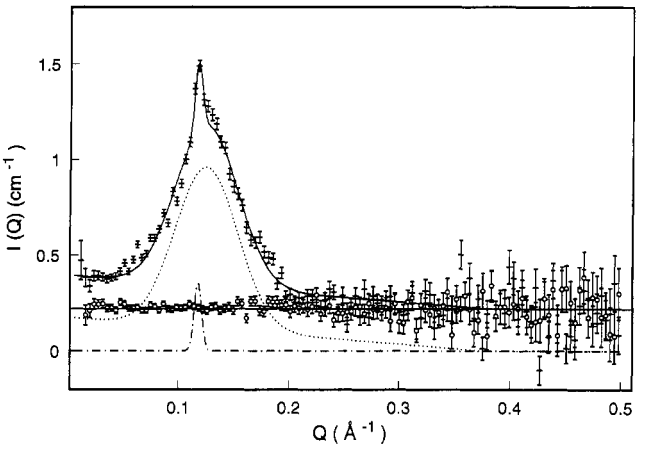

FIGURE 1: Neutron in-plane scattering of alamethicin inserted in DLPC bilayers at molar ratio P:L = 1:10 and hydrated with D_2O (data +). After the sample was exposed to H_2O vapor for 48 h, the neutron scattering was reduced to a constant incoherent background (data O). The error bars represent statistical uncertainties. The scattering curve (+) is decomposed into the incoherent background (straight solid line), a lamellar peak (dash-dot line) due to smectic defects, obtained by a gaussian fit to the sharp peak at $Q \sim 0.12$ Å^{-1}, and the scattering curve of alamethicin pores (dotted line). The recombination of these three components (solid curve) agrees very well with the original data. The lamellar peak has the same width as the peak of pure lipid in Figure 2, as expected.

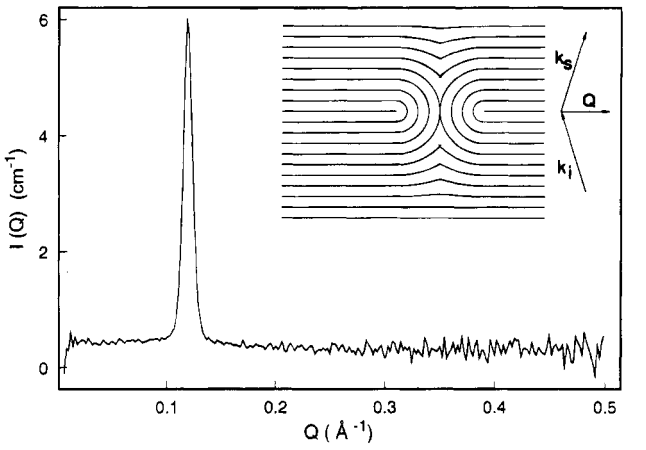

FIGURE 2: Neutron in-plane scattering of pure DLPC bilayers hydrated with D_2O. If the bilayers were perfectly aligned, the scattering intensity should be just the incoherent scattering background, constant in this range of Q. However, in the smectic liquid crystalline phase, some defects (called oily streaks) are inevitable. The inset shows a schematic of molecular planes in an oily streak structure. The white areas are the lipid bilayers, and dark lines represent the water layers. This defect presents a repeating array of bilayers perpendicular to **Q** (k_i represents the momentum of the incident neutron and k_s that of the scattered neutron), which gives rise to a lamellar peak at $Q \sim 0.12$ Å^{-1} corresponding to a repeating distance ~52 Å. The same peak appeared in Figure 1.

dependence until Q is about 2π divided by the molecular diameter measured in the direction of **Q**. In the case of lipid, this is about 1.4 Å^{-1} (He et al., 1993a), and for D_2O it is even higher. However, an oily streak configuration (see the inset of Figure 2) presents a repeating array of bilayers perpendicular to **Q**, which gives rise to the lamellar diffraction peak. The peak at $Q = 0.12$ Å^{-1} corresponds to a lamellar spacing of 52 Å, indicating that the sample was well hydrated (Wu et al., 1995). In Figure 1, this peak and a constant incoherent background are removed from the raw data to obtain the in-plane scattering of inserted alamethicin in DLPC bilayers (Figure 3).

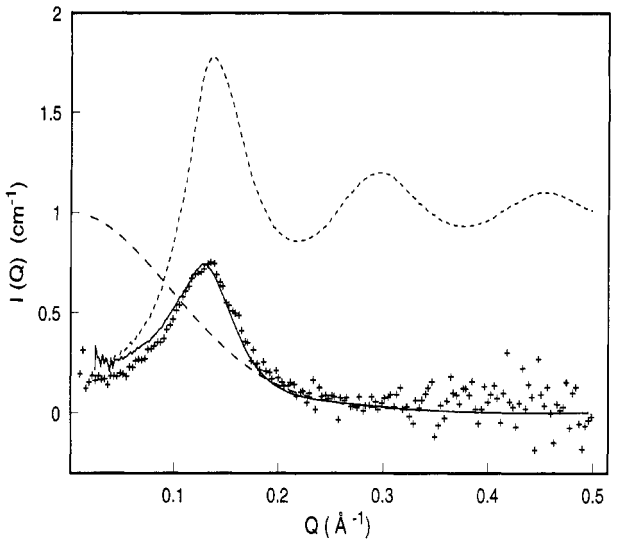

FIGURE 3: Scattering curve of alamethicin pores (data +) was obtained by subtracting the incoherent background and the lamellar peak from the original data of Figure 1. Short-dashed line is the simulated structure factor $S(Q)$ for eight-monomer pores, assuming that all of the peptide at P:L = 1:10 forms such pores. Long-dashed line is the square of the corresponding form factor, $|F(Q)|^2$. Solid line is the product $|F(Q)|^2S(Q)$ to be compared with the data.

DISCUSSION

We interpret the scattering curve (Figure 3) with a model schematically shown in Figure 4. The inserted peptide forms discrete pores in the barrel-stave fashion, as originally proposed for the alamethicin channels detected by single-channel ion conduction techniques (Baumann & Mueller, 1974). The scattering length densities of DLPC, alamethicin, H_2O and D_2O are, respectively, 0.35, 1.8, −0.56, and 6.35 in units of 10^{10} cm^{-2} (Bacon, 1975). With **Q** in the plane of the bilayer, the D_2O within the pore provides the primary contrast against the lipid background. When the D_2O was replaced by H_2O (by exposing the sample to H_2O vapor), the contrast became sufficiently small that the signal was not distinguishable from a constant incoherent background (recall that the instensity is proportioanl to the square of the contrast; see Figure 1). This proves that water is part of the high-order structure of the inserted peptide. It also shows that the peptide's contribution to the scattering is negligible in the region of Q where the scattering is observed.

It is relatively straightforward to analyze the scattering curve shown in Figure 3. The basic law of scattering is well-known (Bacon, 1975). For in-plane scattering, the scattering intensity $I(Q)$ as a function of Q is given by (He et al., 1993a)

$$I(Q)/N = |F(Q)|^2S(Q) \quad (1)$$

with

$$S(Q) = 1 + \int[\rho_c(r) - \bar{\rho}]J_o(Qr)2\pi r\,dr \quad (2)$$

where $S(Q)$ is the structure factor, N the number of pores, $F(Q)$ the scattering amplitude by an individual pore, called the form factor, $\rho_c(r)2\pi r\,dr$ the average number of pores within the ring of radius r and width dr, centered at an arbitrarily chosen pore, $\bar{\rho}$ the mean number density of pores, and $J_o(Qr)$ the zeroth order Bessel function of Qr. Generally speaking, the form factor is sensitive to the molecular configuration of the scattering object, and the

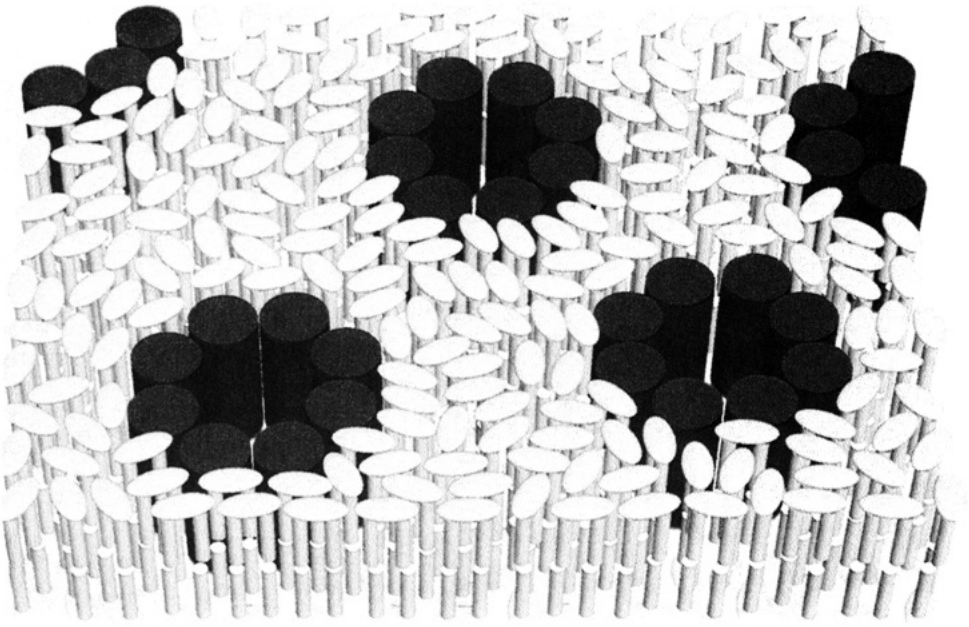

FIGURE 4: Schematic of alamethicin pores in DLPC bilayer. The pore is made of eight alamethicin monomers in the barrel-stave fashion. Each monomer is represented by a cylinder of about 11 Å in diameter. The outer diameter of the pore is about 40 Å. The diameter of the water pathway is about 18 Å. Lipid molecules (two-legged objects) are drawn approximately to scale. The surface density of pores roughly correspond to peptide to lipid molar ratio 1:10.

structure factor is sensitive to the size of the scattering object and the interaction potential between the objects. The presence of a scattering peak tells us that we have well-defined scattering objects. And the peak position (Q_{max}) alone gives us a rough measure of their size (He et al., 1993a,b). Using this estimate, the outside diameter of the pores is about $2\pi/Q_{max} \sim 49$ Å.

For quantitative analysis, the scattering curve can be simulated using circular cylinders to represent the pores. We assume that the cylinder is lined by n alamethicin helices in the barrel-stave fashion, leaving a cylindrical water pathway in the middle. From the molecular dimensions of an alamethicin monomer (Fox & Richards, 1982), the outside diameter, $2R$, and inside diameter, $2r$, can be estimated. Since the molecular cross sections of lipids are also known (Wu et al., 1995), the total area of the membrane containing N cylinders can be estimated from the peptide to lipid ratio. We let 1000 cylinders diffuse randomly within the area with the constraint that no two cylinders can overlap with each other. After the system reached equilibrium, the structure factor $S(Q) = |\sum_j \exp(i\mathbf{Q}\cdot\mathbf{r}_j)|^2$, where $\mathbf{r}_j$ is the position of the center of the jth cylinder, was computed and averaged over time. In Figure 3 we show that the $S(Q)$ for cylinders of eight monomers multiplied by the square of the corresponding form factor $F(Q)$ agrees well with the data. In this example, the peptide's contrast against the lipid background is small, so $F(Q)$ is most sensitive to the radius of the aqueous pore, r. However the peptide contributes to the scattering by limiting the distance of closest approach. Indeed $S(Q)$ is most sensitive to the outside radius R (He et al., 1993b). As a result, both the radii of the aqueous pore and the channel are determined quite accurately (±1 Å). In a previous study on in-plane scattering (He et al., 1993b), we have shown that the peak width and peak amplitude of the structure factor are sensitive to the density of the scattering object. The neutron data are consistent with the assumption that all of the alamethicin at P:L = 1:10 is involved in pore formation. To test the sensitivity to the

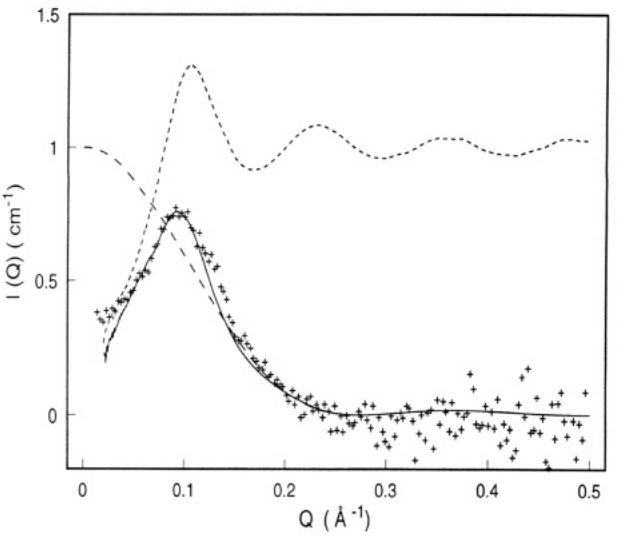

FIGURE 5: Scattering curve of alamethicin pores in DPhPC bilayers at molar ratio P:L = 1:10. The data (+) are compared with the simulated scattering curve of pores made of 11 alamethicin monomers. The short-dashed line is $S(Q)$, the long-dashed line $|F(Q)|^2$, and the solid line $|F(Q)|^2S(Q)$.

pore size distribution, we simulated cylinders of seven monomers, cylinders of nine monomers, and cylinders of sizes following a gaussian distribution centered at eight monomers. We conclude that alamethicin forms pores in a narrow range of size. Most of them (>70%) are made of n and $n \pm 1$ monomers. In DLPC at P:L = 1:10, the mean size n is 8. The effective outside diameter of the pores ($2R$) is ~40 Å, with an aqueous pore of ~18 Å in diameter ($2r$) as schematically shown in Figure 4. The size of the pores appears to vary somewhat with the water content. It also varies with lipid. In DPhPC at P:L = 1:10, the mean size n is about 11 (Figure 5). The effective outside diameter of the pores is ~50 Å, with an aqueous pore of ~26 Å in diameter. Not surprisingly, pores were not detected by in-plane scattering in DPhPC with alamethicin concentrations below CCI (~1:40). Technical details of the experiment and

analysis will be published elsewhere.

The state of alamethicin detected by neutron scattering is quite different from the single-channel behavior of the peptide detected by the patch-clamp or the black-lipid membrane techniques (Baumann & Mueller, 1974; Mak & Webb, 1995). Single channels are measured at extremely low concentrations of peptides. Under such conditions, the great majority of the peptide monomers are adsorbed in the bilayer's headgroup region with their long axes oriented parallel to the surface (Wu et al., 1995), and the single channels are transient fluctuation phenomena. An alamethicin single channel typically fluctuates among five or more levels ranging in size from $n \sim 5$ to 10, with a mean dwell time a fraction of a second at each level and a total lifetime in minutes (Mak & Webb, 1995). The main effect of the adsorbed peptide is reducing the thickness of the hydrocarbon region of the bilayer, directly proportional to P:L (Wu et., 1995; Ludtke et al., 1995). This has the effect of increasing the free energy of adsorption in proportion to the square of P:L (Huang, 1995). Thus, at sufficiently high concentrations, the energy of adsorption will exceed the energy of insertion, making peptide insertion favorable. Once the majority of the peptide is inserted, the pores are the equilibrium state. Permeabilities of such a high density of pores will most likely exceed the homeostatic capacities of the microorganism. We are now extending the investigation to cecropins and magainins to determine if concentration-dependent pore formation is the common mechanism of the antimicrobial peptides.

ACKNOWLEDGMENT

We thank B. Hammouda, P. Thiyagarajan, and D. G. Wozniak for help with experiments at NIST and at IPNS.

REFERENCES

Asher, S. A., & Pershan, P. S. (1977) *Biophys. J. 27*, 137−152.
Bacon, G. E. (1975) *Neutron Diffraction*, Chapter 16, pp 544−580, Clarendon Press, Oxford.
Baumann, G., & Mueller, P. (1974) *J. Supramol. Struct. 2*, 538−557.
Bechinger, B., Kim, Y., Chirlian, L. E., Gesell, J., Neumann, J.-M., Motal, M. Tomich, J., Zasloff, M., & Opella, S. J. (1991) *J. Biomol. NMR 1*, 167−173.
Boman, H. G., Marsh, J., & Goode, J. A., Eds. (1994) *Antimicrobial Peptides*, Ciba Foundation Symposium 186, John Wiley & Sons, Chichester.
Christensen, B., Fink, J., Merrifield, R. B., & Mauzerall, D. (1988) *Proc. Natl. Acad. Sci. U.S.A. 85*, 5072−5076.
Cruciani, R. A., Barker, J. L., Zasloff, M., Chen, H.-C., & Colamonici, O. (1991) *Proc. Natl. Acad. Sci. U.S.A. 88*, 3792−3796.
Cruciani, R. A., Barker, J. L., Durell, S. R., Raghunathan, G., Guy, R., Zasloff, M., & Stanley, E. F. (1992) *Eur. J. Pharmacol. 226*, 287−296.
Duclohier, H., Molle, G., & Spach, G. (1989) *Biophys. J. 56*, 1017−1021.
Fox, R. O., & Richards, F. M. (1982) *Nature 300*, 325−330.
Gomes, A. V., De Waal, A., Berden, J. A., & Westerhoff, H. V. (1993) *Biochemistry 32*, 5365−5372.
He, K., Ludtke, S. J., Wu, Y., & Huang, H. W. (1993a) *Biophys. J. 64*, 157−162 .
He, K., Ludtke, S. J., Wu, Y., & Huang, H. W. (1993b) *J. Phys. IV 3*, 265−270.
Huang, H. W. (1995) *J. Phys. (Paris)* (in press).
Huang, H. W., & Olah, G. A. (1987) *Biophys. J. 51*, 989−992.
Huang, H. W., & Wu, Y. (1991) *Biophys. J. 60*, 1079−1087.
Hultmark, D., Steiner, H., Rasmuson, T., & Boman, H. G. (1980) *Eur. J. Biochem. 106*, 7−16.
Jen, W.-C., Jones, G. A., Brewer, D., Parkinson, V. O., & Taylor, A. (1987) *J. Appl. Bacteriol. 63*, 293−298.
Juretic, D., Chen, H.-C., Brown, J. H., Morell, J. L., Hendler, R. W., & Westerhoff, H. V. (1989) *FEBS Lett. 249*, 219−223.
Ludtke, S. J., He, K., Wu, Y., & Huang, H. W. (1994) *Biochim. Biophys. Acta 1190*, 181−184.
Ludtke, S. J., He, K., & Huang, H. W. (1995) *Biochemistry* (in press).
Mak, D. D., & Webb, W. W. (1995) *Biophys. J.* (in press).
Matsuzaki, K., Murase, O., Fujii, N., & Miyajima, K. (1995) *Biochemistry 34*, 6521−6526.
Pandey, R. C., Cook, J. C., & Rinehart, K. L. (1977) *J. Am. Chem. Soc. 99*, 8469−8483.
Steiner, H., Andreu, D., & Merrifield, R. B. (1988) *Biochim. Biophys. Acta 939*, 260−266.
Westerhoff, H. V., Hendler, R. W., Zasloff, M., & Juretic, D. (1989) *Biochim. Biophys. Acta 975*, 361−369.
Wu, Y., Huang, H. W., & Olah, G. A. (1990) *Biophys. J. 57*, 797−806.
Wu, Y., He, K., Ludtke, S. J., & Huang, H. W. (1995) *Biophys. J. 68*, 2361−2369.
Zasloff, M. (1987) *Proc. Natl. Acad. Sci. U.S.A. 84*, 5449−5453.

BI9521046